Inorganic Chemistry
Article

Inorg. Chem. **2009**, *48*, 10635–10642 **10635**
DOI: 10.1021/ic901165j

Reaction Sequence and Kinetics of Uranium Nitride Decomposition

G. W. Chinthaka Silva,[†] Charles B. Yeamans,[‡] Alfred P. Sattelberger,[†,§] Thomas Hartmann,[†] Gary S. Cerefice,[†] and Kenneth R. Czerwinski*[,†]

[†]*Harry Reid Center for Environmental Studies, University of Nevada, Las Vegas, Box 454009, 4505 Maryland Parkway, Las Vegas, Nevada 89154,* [‡]*Department of Nuclear Engineering, University of California, Berkeley, 4155 Etcheverry Hall, M.C. 1730, Berkeley, California 94720-1730, and* [§]*Energy Sciences and Engineering Directorate, Argonne National Laboratory, 9700 Cass Avenue, Building 208, Argonne, Illinois 60439*

Received June 17, 2009

The reaction mechanism and kinetics of the thermal decomposition of uranium dinitride/uranium sesquinitride to uranium mononitride under inert atmosphere at elevated temperature were studied. An increase in the lattice parameter of the $UN_2/\alpha\text{-}U_2N_3$ phase was observed as the reaction temperature increased, corresponding to a continuous removal of nitrogen. Electron density calculations for these two compounds using XRD powder patterns of the samples utilizing charge-flipping technique were performed for the first time to visualize the decrease in nitrogen level as a function of temperature. Complete decomposition of UN_2 into $\alpha\text{-}U_2N_3$ at 675 °C and the UN formation after a partial decomposition of $\alpha\text{-}U_2N_3$ at 975 °C were also identified in this study. The activation energy for the decomposition of the $UN_2/\alpha\text{-}U_2N_3$ phase into UN, 423.8 ± 0.3 kJ/mol (101.3 kcal/mol), was determined under an inert argon atmosphere and is reported here experimentally for the first time.

1. Introduction

Uranium mononitride (UN) has been considered as a potential fuel for Generation IV nuclear reactor systems due to its favorable physical and chemical properties.[1] In particular, fast breeder systems benefit from the higher fissile-atom density in UN as compared to UO_2, and its superior mechanical, thermal, and radiation stability as compared to metallic fuel.[2] Additionally, accelerator-driven subcritical systems for minor-actinide transmutation can also utilize a nitride-based inert matrix fuel.[3] Of the techniques used to synthesize UN from UO_2 for nuclear fuel, carbothermic reduction[4−6] is the most common in industrial applications. Sol−gel methods[3,7] are also proposed for the synthesis of actinide nitrides. In some studies, both sol−gel methods and carbothermic reduction have been used,[8] as has arc-melting of pure uranium metal in a nitrogen atmosphere. Arc-melting results in the formation of a U_2N_{3+x} layer and UO_2 impurity phase.[9] Low-temperature methods include the reaction of uranium carbide (UC)[10,11] and uranium fluoride (UF_4) with ammonia.[12] In a previous study, formation of U_2N_3 was detected when UC was heated in a thermogravimetric balance under N_2.[13]

UN is the lowest-stoichiometry nitride of the U−N solid system, commonly considered to have three distinct compounds: uranium dinitride (UN_2), uranium sesquinitride (U_2N_3), and UN.[14] Higher uranium nitrides decompose to UN by the following sequence of reactions:

$$2UN_2 \rightarrow \alpha\text{-}U_2N_3 + \frac{1}{2}N_2 \quad (1)$$

$$\alpha\text{-}U_2N_3 \rightarrow 2UN + \frac{1}{2}N_2 \quad (2)$$

The UN_2 compound is a face-centered cubic CaF_2-type structure with a space group of $Fm\bar{3}m$ compared to the

*To whom correspondence should be addressed. E-mail: czerwin2@unlv.nevada.edu. Tel: (702) 895 0501. Fax: (702) 895 3094.

(1) Arai, Y.; Minato, K. *J. Nucl. Mater.* **2005**, *344*, 180.
(2) Mizutani, A.; Sekimoto, H. *Ann. Nucl. Energy* **1998**, *25*, 1011.
(3) Streit, M.; Ingold, F. *J. Eur. Ceram. Soc.* **2005**, *25*, 2687.
(4) Arai, Y.; Fukushima, S.; Shiozawa, K.; Handa, M. *J. Nucl. Mater.* **1989**, *168*, 280.
(5) Ogawa, T.; Shirasu, Y.; Minato, K.; Serizawa, H. *J. Nucl. Mater.* **1997**, *247*, 151.
(6) Minato, K.; Akabori, M.; Takano, M.; Arai, Y.; Nakajima, K.; Itoh, A.; Ogawa, T. *J. Nucl. Mater.* **2003**, *320*, 18.
(7) Ganguly, C.; Hegde, P. V. *J. Sol-Gel Sci. Technol.* **1997**, *9*, 285.
(8) Mukerjee, S. K.; Dehadraya, J. V.; Vaida, V. N.; Sood, D. D. *J. Nucl. Mater.* **1991**, *185*, 39.
(9) Sole, M. J.; Van Der Walt, C. M. *Acta. Metall.* **1968**, *16*, 501.
(10) Katsura, M.; Hirota, M.; Miyake, M. *J. Alloys Compd.* **1994**, *213*/*214*, 440.
(11) Katsura, M. *Solid State Ionics* **1991**, *49*, 225.
(12) Silva, G. W. C.; Yeamans, C. B.; Ma, L.; Cerefice, G. S.; Czerwinski, K. R.; Sattelberger, A. P. *Chem. Mater.* **2008**, *20*, 3076.
(13) Hanson, L. A. *J. Nucl. Mater.* **1966**, *19*, 15.
(14) Morss L. R., Edelstein N. M., Fuger J., Katz J. J., Eds. *The Chemistry of the Actinides and Transactinide Elements*, 3rd ed.; Chapman & Hall: New York, 2006; Vol. *1*.

Published on Web 10/21/2009

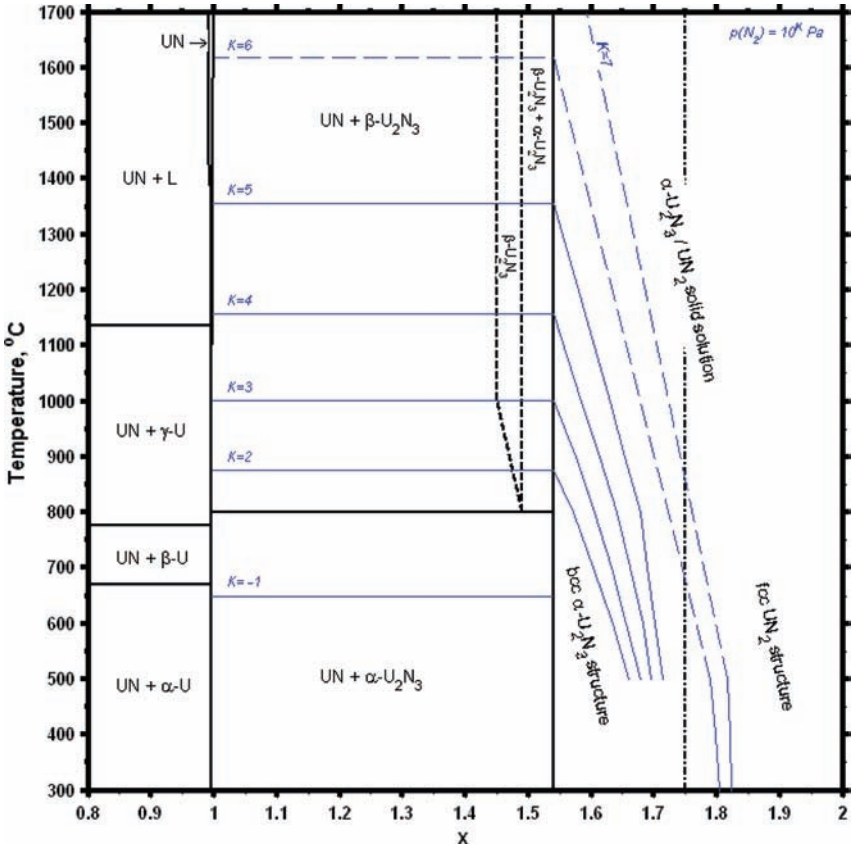

Figure 1. Equilibrium phase diagram of the pure UN_x system.[23]

body-centered cubic Mn_2O_3-type structure of α-U_2N_3 with a $Ia\bar{3}$ space group.[15] The fcc UN_2 structure shows a range of compositions described as UN_x where $2.0 \geq x \geq 1.75$.[16] The UN_2/α-U_2N_3 system forms stable solid solutions at all intermediate compositions above $UN_{1.54}$[17] while reports indicate up to 1.45 N/U molar ratio for the α-U_2N_3 composition. In these solid solutions, a continuous change of the uranium and nitrogen atomic positions within the unit cell with composition is also reported.[16,17] As a result, the names "UN_2" and "U_2N_3" are often applied interchangeably to the UN_2/α-U_2N_3 solid solution chemical phase. Since the apparent crystallographic change from CaF_2-type face-centered cubic UN_2 to Mn_2O_3-type body-centered cubic α-U_2N_3 occurs at a composition of $UN_{1.75}$,[18] it is common to refer to solutions with stoichiometry above $UN_{1.75}$ as UN_2 and below it as α-U_2N_3. That common convention will be used in this report for the sake of consistency with previous studies.

We find that the higher-stoichiometry uranium nitrides are more stable than UN toward adventitious amounts of oxygen present in our experimental setups.[12,19] The higher nitrides are actually synthesized at lower temperatures than UN,[5,20] which contribute to their greater apparent oxygen-stability according to the observations previously reported.[12] The current work also observed the formation of a UO_2 secondary phase up to 10 wt % in UN, whereas only minor levels of UO_2 (up to 1 wt %) were identified in UN_2 and U_2N_3 samples. Pure UN is always slightly substoichiometric, and has a maximum nitrogen-rich composition of $UN_{0.995}$ at 1100 °C and below.[21] Small oxygen impurities (< 1 wt %) stabilize α-U_2N_3 at higher temperatures,[22] so the apparent equilibrium at intermediate compositions in the U−N system is between $UN_{1.45}$ and $UN_{0.995}$, having the common designations α-U_2N_3 and UN, respectively, as long as some oxygen impurities are present. A phase diagram for the UN_x system is shown in Figure 1 to provide detail.

Even though a number of reports exist on the presence of these different uranium nitrides under various experimental conditions and physical properties, there is little information available on the reaction kinetics associated with the formation of UN from UN_2 or α-U_2N_3. The current study focuses on confirming that the aforementioned decomposition reaction sequence (eqs 1 and 2) is correct, and determining the relevant kinetic parameters and activation energies. Formation temperatures of α-U_2N_3 and UN were identified by systematically decomposing UN_2 at various temperatures under an inert argon atmosphere. The kinetics of these reactions was analyzed using a pseudo-first-order model because it shows relatively better match to the experimental results compared to a zero-order analysis. Arrhenius plots were generated to determine the activation energies.

(15) Rundle, R. E.; Baenziger, N. C.; Wilson, A. S.; McDonald, R. A. *J. Am. Chem. Soc.* **1948**, *70*, 99.
(16) Tagawa, H. *J. Nucl. Mater.* **1974**, *51*, 78.
(17) Serizawa, H.; Fukuda, K.; Ishii, Y.; Morii, Y.; Katsura, M. *J. Nucl. Mater.* **1994**, *208*, 128.
(18) Tagawa, H.; Masaki, N. *J. Inorg. Nucl. Chem.* **1974**, *36*, 1099.
(19) Yeamans, C. B.; Silva, G. W. C.; Cerefice, G. S.; Czerwinski, K. R.; Hartmann, T.; Burrell, A. K.; Sattelberger, A. P. *J. Nucl. Mater.* **2008**, *374* (1−2), 75.
(20) Mallett, M. W.; Gerds, A. F. *J. Electrochem. Soc.* **1955**, *102*(6), 292.
(21) Hoenig, C. L. *J. Am. Chem. Soc.* **1971**, *54*, 391.
(22) Benz, R.; Balog, G.; Baca, B. H. *High Temp. Sci.* **1970**, *2*, 221.

2. Experimental Details

2.1. Uranium Nitride Synthesis. Ammonolysis of UF_4 was used to synthesize UN_2. A 1015.76 (5) mg sample of UF_4 (International Bio-Analytical Industries, Inc.) was loaded in a quartz-glass boat wrapped with platinum foil and placed inside a 25.4 mm diameter quartz-glass tube, capped on either end with 25 mm quartz-glass Solv-Seal fittings (Andrews Glass Co., Inc.). Pyrex Solv-Seal caps fitted with 15 mm high vacuum Teflon stopcocks sealed the tube and allowed a controlled atmosphere to blanket the sample. The sample was held at 800 °C for 1 h under ammonia gas (research grade, Praxair) after which 858.53 (5) mg of UN_2 was obtained. The mass loss for the transformation of UF_4 into UN_2 was 157.23(5) mg. This indicates an extra 2 mg mass loss compared to the expected value of 155.2 mg. This extra additional mass loss is attributed to errors associated with the experimental measurements. A 218.74 (5) mg sample of α-U_2N_3 was synthesized by decomposing 225.35 (5) mg of the synthesized UN_2 under an inert atmosphere (ultrahigh purity argon, 99.9999%, Praxair) at 700 °C for 1 h. The mass loss was 6.6 mg which is relatively close to the expected value of 5.9 mg. Batches of different UN_2 and α-U_2N_3 masses were used to synthesize UN to determine the reaction kinetics and temperature effects. A detailed description of these nitrides syntheses can be found in previous publications.[12,19]

2.2. Characterization Methods. X-ray powder diffraction (XRD) patterns were obtained using a Philips PANalytical X'Pert Pro instrument with a Ni-filtered Cu Kα radiation. The patterns were collected using 40 mA current and 40 kV tension at room temperature. Chemical phases in the samples were initially determined matching the XRD powder patterns with the International Center for Diffraction Data (ICDD) database patterns. Following are the reference patterns used for separate compounds: UN_2 (01-073-1713), U_2N_3 (01-073-1712), UN (00-032-1397), and UO_2 (00-041-1422). An internal LaB_6 standard from NIST (SRM 660a) was admixed with the uranium nitride samples to allow for precise lattice parameter refinement and to optimize the quality of Rietveld analysis as performed.

Electron density maps of uranium nitrides were calculated using the XRD powder patterns of the samples. Le Bail decomposition[24] was used to extract the individual observed structure factor amplitudes (F_{obs}) of the XRD powder pattern using Jana2000.[25] These observed structure factors were then used to calculate the electron density maps of the compounds by the charge-flipping algorithm through the Superflip program.[26] The calculated electron density maps were visualized using UCSF Chimera.[27] A Tecnai-G2-F30 supertwin transmission electron microscope system with a 300 keV Schottky field emission gun was used in TEM imaging. Bright field (BF) and the high resolution (HRTEM) modes of TEM were utilized in sample characterization. All TEM images were recorded using a slow scan CCD camera attached to a Gatan GIF 2000 energy filter.

3. Results

3.1. UN_2 Decomposition. The thermal behavior of UN_2 in an inert atmosphere was determined by heating three UN_2 samples of approximately 50 mg each at 500, 700, and 1100 °C under flowing high-purity argon (99.9999%) for 30 min. Heating the first sample at 500 °C resulted in no measurable decomposition of the UN_2. At 700 °C, UN_2 was completely converted to α-U_2N_3. After heating at 1100 °C for 30 min, the only uranium nitride phase identified in the samples was UN. The latter sample also contained a 5.3 (1) wt % secondary UO_2 phase, most likely due to trace oxygen contamination in the experimental system. Subsequent experiments were conducted in two different temperature ranges of 500−700 °C and 700−1100 °C (Table 1) to refine the temperatures in which the decomposition reactions in eqs 1 and 2 occur. At each of these temperatures, the reactants were heated for 30 min initially to determine where the decomposition reactions occur. These experiments showed that the UN_2 decomposition to α-U_2N_3 starts at about 675 °C, and the second decomposition to UN begins near 975 °C. Therefore, the decompositions at 650 and 950 °C were studied further with up to 60 min of heating. These two experiments showed neither formation of α-U_2N_3 at 650 °C nor formation of UN at 950 °C. Heating of UN_2 at 600 and 900 °C was also conducted for up to 240 min to determine how duration would affect UN_2 decomposition. At 600 °C (a = 0.53050(6) nm), no α-U_2N_3 formation occurred. No UN formation was perceived at 900 °C as well (a = 1.068890(7) nm). Even though no phase transformations were observed, increase in the lattice parameters of UN_2 and α-U_2N_3 was detected as described in Figure 2. Also, over the temperature range from 975 to 1100 °C, both α-U_2N_3 and UN were observed in the product.

Table 1. Products Observed after Heating UN_2 at Different Temperatures and Time Intervals under Argon

temperature (°C)	time of heating (min.)	products observed
500	30	UN_2
600	30	UN_2
	240	UN_2
650	30	UN_2
	60	UN_2
675	30	U_2N_3
700	30	U_2N_3
750	30	U_2N_3
800	30	U_2N_3
900	30	U_2N_3
	240	U_2N_3
950	30	U_2N_3
	60	U_2N_3
975	30	U_2N_3, UN
1000	30	U_2N_3, UN
1050	30	U_2N_3, UN
1100	30	UN

The refined lattice parameters of UN_2 and U_2N_3 were shown to vary with respect to the temperature (Figure 2). Lattice parameters of both these nitrides change linearly as a function of temperature. A 0.0004 nm change was determined in the lattice parameter of UN_2 over a 150 °C temperature range. The lattice parameter change determined for the α-U_2N_3 samples over a 275 °C temperature range was about 0.004 nm, a 6-fold increase compared to the change of the UN_2 lattice parameter relative to the final lattice parameter of each compound. Possible reasons for this observation are discussed in the following paragraph using electron microscopic characterizations.

(23) Yeamans, C. B. Synthesis of Uranium Fluorides from Uranium Dioxide with Ammonium Bifluoride and Ammonolysis of Uranium Fluorides to Uranium Nitrides. Ph.D. dissertation. University of California, Berkeley, Berkeley, California, 2008,; pp 12−18.

(24) Bail, A. Le.; Duroy, H.; Fourquet, J. L. *Mater. Res. Bull.* **1998**, *23*, 447−452.

(25) DusÏek, M.; PetrÏõÂcÏek, V.; Wunschel, M.; Dinnebier, R. E.; van Smaalen, S. *J. Appl. Crystallogr.* **2001**, *34*, 398−404.

(26) Palatinus, L.; Chapuis, G. *J. Appl. Crystallogr.* **2007**, *40*, 786−790.

(27) Pettersen, E. F.; Goddard, T. D.; Huang, C. C.; Couch, G. S.; Greenblatt, D. M.; Meng, E. C.; Ferrin, T. E. *J. Comput. Chem.* **2004**, *25* (13), 1605−1612.

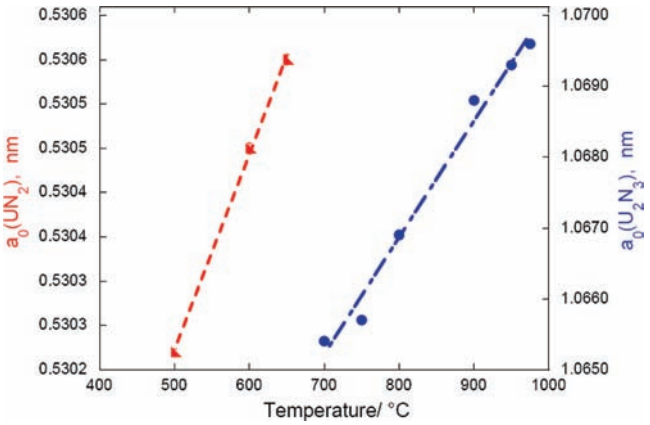

Figure 2. Lattice parameters of UN_2 and α-U_2N_3 as a function of the temperature used for decomposition.

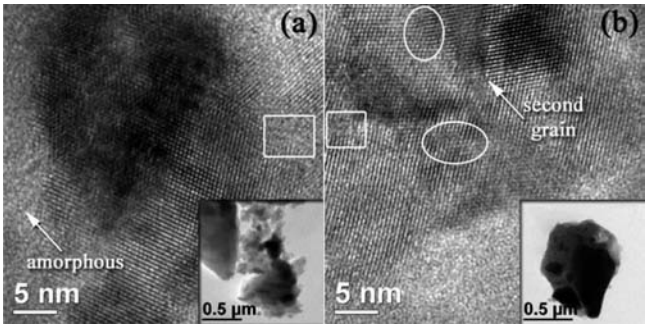

Figure 3. HRTEM images of UN_2 particles. Insets are the BF images of the particles used in the HRTEM imaging. Squares indicate amorphous areas while circled areas demonstrate disruptions with some amorphous characteristics especially in the lower end circle.

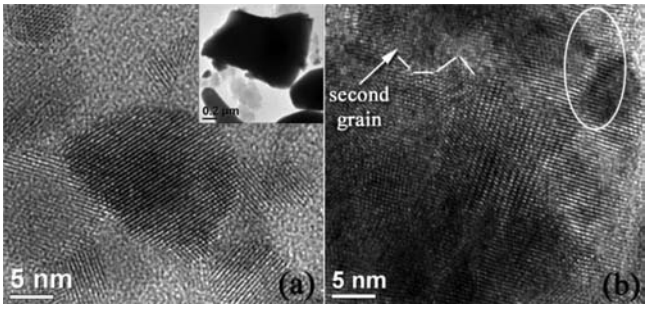

Figure 4. HRTEM images of U_2N_3 particles shown in the inset (the BF image). Circle shows a disrupted nanoparticle area.

HRTEM images of both UN_2 (Figure 3) and U_2N_3 (Figure 4) micro particle areas presented here contained some deformations in their nanostructures. In the case of UN_2, bulk particle areas included single crystal characteristics. However, some of these grains had amorphous areas as shown in Figure 3a (with an arrow and the rectangle box). As a specific example, a single crystal particle (inset of Figure 3b) exhibited some disruptions at the nanoscale. These abnormal observations are highlighted in Figure 3b. These nanostructural disorders occur either from the specimen preparation techniques or the formation of a secondary phase. If the first reason is dominant, these disruptions should extend up to bulk particle areas and such large disruptions could not be observed (inset of Figure 3b). The lattice fringes do not represent a secondary UO_2 phase in the nano particle

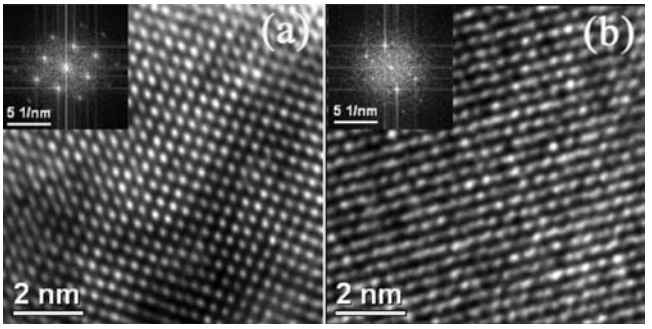

Figure 5. HRTEM images of UN_2 (a) and U_2N_3 (b). Insets are the corresponding FFT micrographs of each HRTEM image.

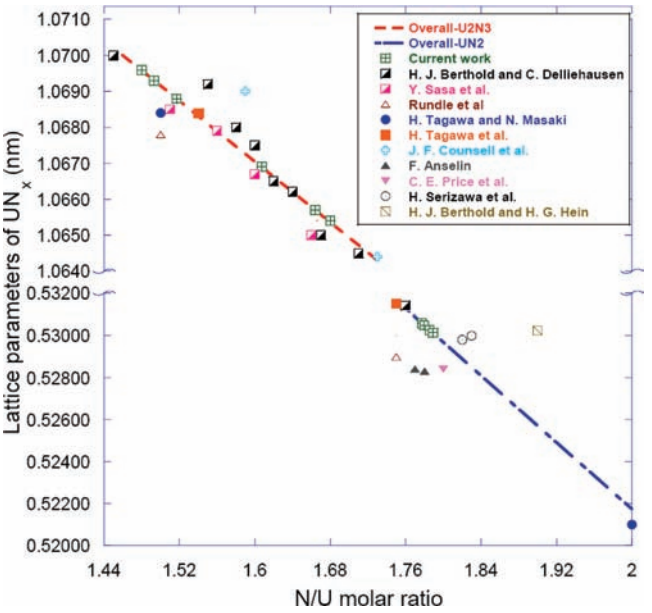

Figure 6. Change in the lattice parameter of the UN_2/α-U_2N_3 system with respect to the N/U molar ratio.

areas of the imaged particle. Therefore, the disorders identified in these samples at nanoscale are due to a second phase other than UO_2. Because UN_x represents a range of "x" values, another UN_x with different chemical composition compared to the main chemical phase in the sample is the probable reason for such nanostructural disruptions. Presence of another minor UN_x phase within the main UN_2 is therefore the reason for the solid solution characteristics in the sample. These separate phases could not be differentiating from the XRD powder patterns but rather from the nanostructural changes or with lattice parameter changes in the compound. Therefore, these nanostructural changes in UN_2 are due to a UN_x phase inferring in solid solution characteristics. Change in the UN_2 lattice parameter as a function of temperature implying the range of compositions of UN_x present (Figure 2) also supports the observation of solid solution behavior. The U_2N_3 sample also showed similar solid solution behavior from its nanostructure characteristics. Observation of nanosized crystalline domains (Figure 4a) and nanostructural disruptions (Figure 4b) due to dislocations of atomic layers and incomplete crystallization of grains at this scale in some of the U_2N_3 particle areas verify this presumption. Presence of nanosized crystalline domains

smaller than that of the UN_2 also denotes a lower particle crystallization of U_2N_3 than that of UN_2. Low point-to-point resolution of the nanostructure of U_2N_3 depicted in Figure 5b compared to that of UN_2 in Figure 5a supports this observation. Low crystallization of the sample and the presence of small crystalline domains in U_2N_3 suggest a faster change in structure with respect to the temperature than that of UN_2 explaining the larger change in the lattice parameter of U_2N_3 as a function of temperature compared to UN_2 as mentioned above. This behavior should also promote formation of UN from the U_2N_3 phase at elevated temperatures such as 1000 and 1100 °C because UN forms more crystalline[12] chemical phase with a low degree of solid solution behavior with the U_2N_3 precursor.

Table 2. Approximated N/U Molar Ratios Determined for UN_x Samples from Correlation Plots in Figure 6

temperature (°C)	lattice parameter: a (nm)	estimated N/U molar ratio
500	0.53027 ± 0.00003	1.765
600	0.53050 ± 0.00006	1.757
650	0.53060 ± 0.00006	1.753
700	1.06540 ± 0.00014	1.678
750	1.06570 ± 0.00008	1.664
800	1.06690 ± 0.00011	1.607
900	1.0688 ± 0.0006	1.517
950	1.06930 ± 0.00011	1.493
975	1.0696 ± 0.0002	1.479

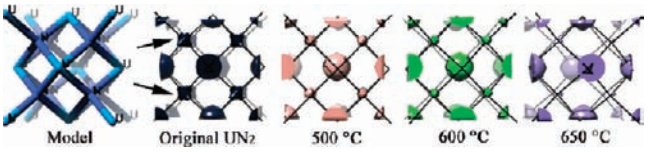

Figure 7. Average electron density maps of UN_2 calculated from XRD powder patterns. Same density level was used in all the images for comparison. A model of the UN_2 unit cell in [001] direction is also shown at the beginning of the series.

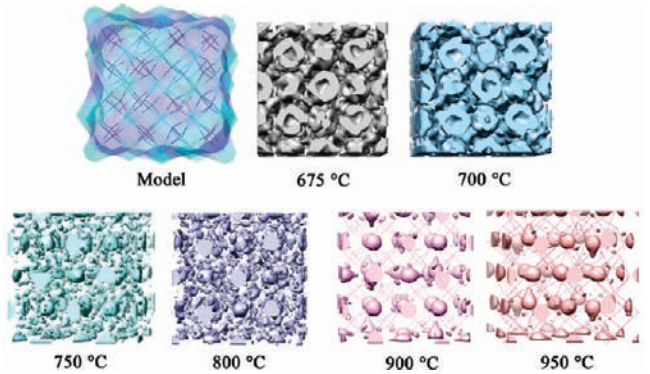

Figure 8. Average electron density maps of U_2N_3 unit cell in the [001] direction.

The N/U molar ratios of these UN_x samples were estimated by correlation plots for UN_2 and α-U_2N_3 (Figure 6).[15−18,28−33] A value of 0.521 nm was taken as the lattice parameter of the stoichiometric UN_2 by assuming behavior analogous to AmO_2 as previously employed by Tagawa et al.[18] The lattice parameter values of the UN_2 samples synthesized and annealed up to 650 °C correlated with those found for samples with approximate N/U molar ratios of 1.75−1.8. However, a lack of data for the UN_x system in the $1.8 \leq x \leq 2.0$ region may imply a higher error in the N/U molar ratio estimations compared to the $1.45 \leq x \leq 1.75$ region. Lattice parameters of α-U_2N_3 samples synthesized in this study show variation comparable to that seen by other authors. Approximate N/U molar ratios determined using the correlation plots in Figure 6 for UN_2 and α-U_2N_3 are summarized in Table 2.

Figure 7 shows a model of UN_2 unit cell together with the average electron density maps in the [001] direction. The electron density at nitrogen positions decreases as the temperature is increased. The decrease in N/U molar ratio with respect to the sample temperature is thus supported by these electron density maps calculated from XRD powder patterns of the samples.

Electron density maps of U_2N_3 samples were also calculated (Figure 8). Due to the complex nature of the U_2N_3 unit cell as indicated in the model, observation of the decrease in average electron density at nitrogen positions could not be easily observed as in UN_2. A close-packed space filling of U_2N_3 unit cell was identified in the electron density maps of first two samples synthesized at 675 and 700 °C. Samples synthesized at 750−950 °C showed more loose packing characteristics of the unit cell

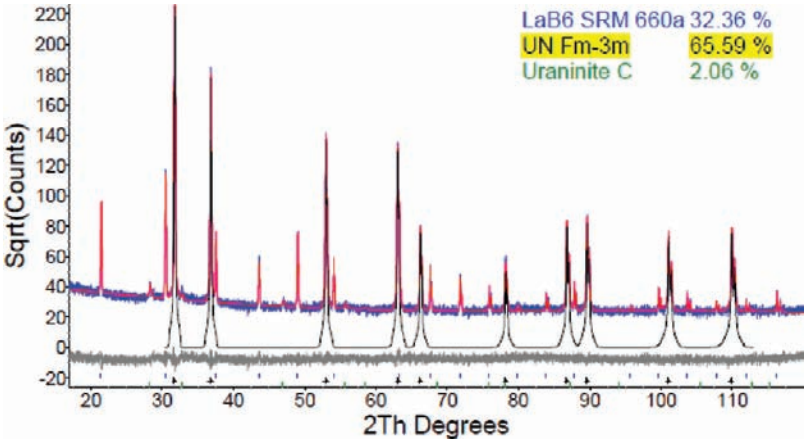

Figure 9. XRD powder refinement of the UN (97 wt %) sample synthesized by heating a UN_2 sample at 1100 °C for 23 min under an inert atmosphere. Highlighted is the calculated pattern of UN.

indicating low density. At 750 and 800 °C temperatures, the samples contain comparatively high electron density at nitrogen atom locations. The electron density decreased when the temperature was raised to 900 or 950 °C. Thus, a reduction of U−N bonding characteristics due to a decrease in the N/U molar ratio can be seen when the temperature is increased in the sample synthesis. These density maps calculated correlate with the observed reaction speciation.

A number of UN samples were synthesized by decomposing UN_x at different temperatures. Secondary chemical phases, including a UO_2 impurity phase (< 10 wt. %) and the incompletely decomposed α-U_2N_3 phase were observed in these samples. The UN samples prepared by decomposition of the UN_2 at 1050 and 1100 °C showed greater product phase content than samples prepared at 975 and 1000 °C due to the presence of larger amounts of incompletely decomposed α-U_2N_3 phase at the lower temperatures. The UO_2 phase impurity was typically less than 5 wt. % at 1100 °C (Figure 9). A plot of the lattice parameters of these UN samples as a function of temperature is shown in Figure 10. The overall change in lattice parameter of UN synthesized at the reported four different temperatures in Figure 10 is about 0.0001 nm. At 975 °C, in which the lowest UN wt. % was observed, the lattice parameter of UN was the highest. At other three temperatures, UN shows a range of lattice parameters even with high phase wt. % at 1100 °C. These observations demonstrate a distribution of the UN lattice parameter over a considerably wide range even at one specific temperature, as was reported elsewhere confirming the formation of UN and its behavior with respect to temperature.[33] Furthermore, no intermediate chemical phases such as β-U_2N_3 were identified between UN and α-U_2N_3 explaining such a variation of lattice parameter of UN phase. Absence of such an intermediate phase was confirmed by heating UN_2 at temperatures near 1000 °C (Table 3) for different time periods. In these experiments no additional phases other than UO_2 were observed. Another experiment illustrated that heating UN_2 under a N_2−H_2 mixture (8% H_2) for 30 min at 1100 °C, for an effective nitrogen pressure of about 92 kPa, produced α-U_2N_3 with no trace of UN. This is consistent with the species predicted by the phase diagram in Figure 1 near the $K = 5$ (N_2 pressure $= 10^5$ Pa) isobar at 1100 °C.

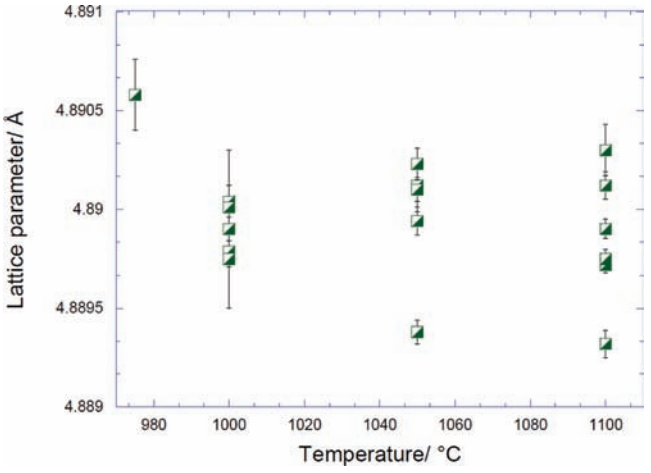

Figure 10. Lattice parameter of UN as a function of the temperature used for decomposition.

Table 3. Phase Distribution of the UN_2 Sample after Heating It at 1000 °C for Different Time Periods

	phase distribution (wt%)		
time (min.)	UN	U_2N_3	UO_2
30	4.9	95.1	
120	17.3	82.7	
240	79.4	18.4	2.2
300	75.0	22.6	2.4
360	76.3	20.5	3.2

3.2. Kinetics of UN_2 Decomposition. UN_2 decomposition studies revealed that α-U_2N_3 formed at temperatures between 675 and 975 °C. Due to the solid solution

Table 4. Rate Constants of the UN_x Decomposition Reaction at 1000, 1050, and 1100 °C

temperature (°C)	rate constant: k ($s^{-1} \times 10^3$)	ln (k /10^{-6} s^{-1})
1000	0.07 ± 0.01	4.22 ± 0.16
1050	0.21 ± 0.02	5.37 ± 0.10
1100	1.3 ± 0.3	7.14 ± 0.24

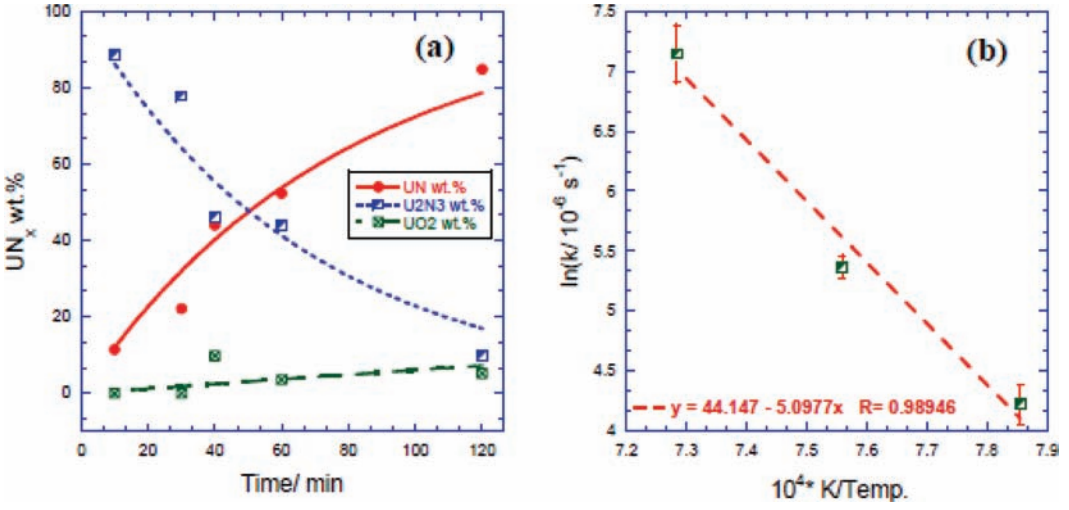

Figure 11. Pseudo-first-order kinetics of UN_x decomposition at 1050 °C (a) and Arrhenius plot for the reaction (b).

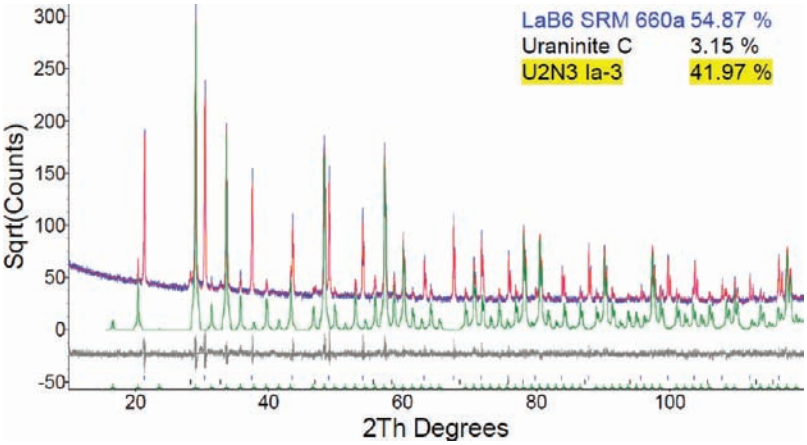

Figure 12. XRD powder refinement of U_2N_3 sample after heating it at 1100 °C for 30 min under N_2- 8% H_2. The U_2N_3 calculated pattern is highlighted.

behavior of UN_2 and U_2N_3 and overlapping peaks in the XRD, the kinetics of this decomposition reaction could not be determined. For the conversion of UN_2/α-U_2N_3 to UN, the reaction kinetics was evaluated at temperatures of 1000, 1050, and 1100 °C. The kinetic data associated with this unimolecular reaction at 1050 °C are shown in Figure 11a, revealing an approximate match between the growth of UN and the decay of α-U_2N_3. Pseudo-first-order was used in determining the kinetics involved in the UN formation since it correlates well with the exponential growth of UN. The zero-order is not valid in this case since at a given time the amount of UN formed was not always a constant value but it was a function of the amount of UN_2 used at the beginning of each experiment. The slight deviation observed in Figure 11 is attributed to the formation of the secondary UO_2 chemical phase. These observations suggest the transition through an intermediate chemical phase of α-U_2N_{3-x}, likely having the uranium-rich boundary composition of $UN_{1.54}$ that reaches a steady-state concentration close to zero. Similar behavior was found for the samples decomposed at 1000 and 1100 °C. Figure 11b displays the Arrhenius plot for this decomposition reaction, and activation energy of 423.8 ± 0.3 kJ/mol was determined. Table 4 summarizes the rate constants determined in the experiment.

4. Discussion

Decomposition of UN_2 under inert atmospheric conditions forms α-U_2N_3 and UN. Obtained XRD patterns for UN_2 and α-U_2N_3 showed single-phased characteristics of the product, with minimal secondary oxide chemical phases. The UN product, however, showed significant phase impurities, with secondary phase levels of UO_2 approaching 10 wt. %. Depending on the decomposition time and conditions, α-U_2N_3 phases, due to incomplete decomposition, were also present up to 80 wt %. Given a heating time between 30 and 240 min, three primary temperature stability regions for the UN_x were identified. The UN_2 phase is the only species present at temperatures less than 675 °C. In the second temperature region, 675−975 °C, UN_2 completely decomposes to α-U_2N_3. Between 975 and 1100 °C, both UN and α-U_2N_3 were detected depending on the temperature and time of heating, with UN being the stable phase in the higher end of the region.

Higher crystallinity of UN_2 in its nanostructure was identified by HRTEM imaging compared to that of U_2N_3. Solid solution behavior of the UN_2 and U_2N_3 samples respectively in the above-mentioned two temperature ranges was also identified with nanostructural changes of the samples. Lower crystallinity and the larger disruptions of the nanostructure of U_2N_3 compared to UN_2 suggested a rapid change in its crystal structure forming a more and well crystallized chemical phase UN. This explains why the lattice parameter in the UN_x system changed much more rapidly above 675 °C. The result supports the conclusion that the reduction of the N/U ratio through decomposition of the UN_x system is kinetically favorable at elevated temperatures. This effect is large enough that even though UN is thermodynamically favorable at a lower temperature, higher-composition UN_x phases are kinetically stable up to 675 °C. A linear increase of the lattice parameters as a function of reaction temperature was measured for both UN_2 and α-U_2N_3 using room temperature XRD. This indicates a continuous removal of nitrogen from the UN_x system, lowering the N/U molar ratio per the correlation reported in Figure 6. Average electron densities calculated on UN_2 and U_2N_3 also showed a decrease of nitrogen in the samples with respect to the increase in temperature confirming the above observation. Heating both UN_2 and U_2N_3 under N_2-8% H_2 for 30 min, even at 1100 °C, produces only α-U_2N_3 (Figure 12). Given that UN_2 and α-U_2N_3 have solid solution behavior, formation of α-U_2N_3 under N_2 at 1100 °C was expected. If any external N_2(g) pressure was introduced during the decomposition of the higher uranium nitrides, removal of nitrogen from the UN_x is difficult and may require temperatures greater than 1100 °C as well as heating times above 30 min.

In contrast to the α-U_2N_3/UN_2 samples, UN showed no distinct pattern in the variation of lattice parameter as a function of reaction temperature. This is consistent with the knowledge that UN has a very narrow range of compositions at temperatures below 1200 °C.[21] Also, considerable levels of uranium oxide impurity (up to about 10 wt. %) had only a small effect on the lattice parameter of the UN phase.

(28) Berthold, H. J.; Delliehausen, C. *Angew. Chem. Int.* **1966**, *5*, 726.
(29) Sasa, Y.; Atoda, T. *J. Am. Chem. Soc.* **1970**, *53*, 102.
(30) Counsell, J. F.; Dell, R. M.; Martin, J. F. *Trans. Faraday Soc.* **1966**, *62*, 1736.
(31) Anselin, F. *J. Nucl. Mater.* **1963**, *10*, 301.
(32) Price, C. E.; Warren, I. H. *Inorg. Chem.* **1965**, *4*, 115.
(33) Berthold, H. J.; Hein, H. G. *Angew. Chem. Int. Ed.* **1969**, *8*, 891.
(34) Cordfunke, E. H. P. *J. Nucl. Mater.* **1975**, *56*, 319.

Because oxide phases are known to have a very low solubility in UN[22] this consistency supports the conclusion that the lattice parameter of UN will not vary significantly as a function of oxide impurity levels across a large composition range of the UN/UO_2 system.

The activation energy for the formation of UN under argon atmosphere starting from UN_x with a composition of UN_x with $x \approx 1.75-1.8$ was determined to be 423.8 ± 0.3 kJ/mol. A theoretical study reported −504.2 kJ/mol as the amount of stabilizing energy for a nitrogen atom occupying a lattice site in α-U_2N_3 with a 1.75 N/U molar ratio.[35] This indicates about 504.2 kJ/mol activation energy requirement to decompose the material into UN according to the eq 2, provided the freeing of nitrogen from the lattice and the creation of a vacancy is the rate-determining step. This result provides reasonable agreement with the activation energy calculated for the decomposition of the higher nitrides to UN (423.8 ± 0.3 kJ/mol) determined in this study as well as the pseudo-first-order behavior of the reaction kinetics.

5. Conclusion

The decomposition of UN_2 samples progressed slowly below 675 °C, but showed a rapid rate increase above that temperature. An intermediate α-U_2N_3 phase was seen at temperatures ≥675 °C under inert atmosphere with a negligible nitrogen pressure. The UN was formed at temperatures greater than 975 °C. A continuous removal of nitrogen was observed in the UN_2 decomposition process to α-U_2N_3 and to UN with a continuous crystal structure changes from fcc to bcc and from bcc to fcc. Electron density maps calculated for the higher uranium nitrides also supported the change in lattice parameters and thus the removal of nitrogen from the crystal systems as a function of temperature. The complete decomposition of about 50 mg of UN_x sample to pure UN could be completed in less than 30 min at 1100 °C. The lattice parameter of UN did not vary significantly with changing reaction temperature or purity of the bulk sample. The activation energy for the formation of UN via α-U_2N_3 decomposition under inert atmospheric conditions was determined to be 423.8 ± 0.3 kJ/mol.

Acknowledgment. We thank Dr. Anthony Hechanova for administrating the UNLV Transmutation Research Program under the financial support of the U.S. Department of Energy (Grant DE-FG07-01AL67358). We are indebted to Tom O'Dou and Trevor Low for outstanding laboratory management and radiation safety.

(35) Fujino, T.; Tagawa, H. *J. Phys. Chem. Solids* **1973**, *34*, 1611.